Electronic Supplementary Information (ESI)

Table S1 Hydrogen bond geometry [Å, °] in **1** and **2**.

Compound	D–H···A	H···A	D···A	D–H···A	Symmetry
1	C10–H10···O9′	2.59	3.284	131.9	0.5–x,0.5+y,0.5–z
	C8–H8B···O11′	2.42	3.119	128.8	–0.5+x,1.5–y,0.5+z
	C7–H7···O13′	2.42	3.344	172.3	–0.5+x,1.5–y,0.5+z
	C19–H19B···O14	2.50	3.376	150.4	1–x,1–y,–z
	C17–H17B···O13	2.46	3.269	141.0	
2	C11–H11···O14′	2.55	3.214	128.7	–0.5+x,1.5–y,0.5+z
	C22–H22A···O13′	2.61	3.369	135.7	–x,2–y,–z
	C22–H22B···O1′	2.59	3.391	141.0	–x,2–y,–z
	C20–H20C···O12′	2.62	3.492	151.6	0.5+x,1.5–y,0.5+z
	C7–H7A···O10	2.40	3.035	123.6	
	C14–H14···O11	2.41	3.275	154.8	–1+x,y,z

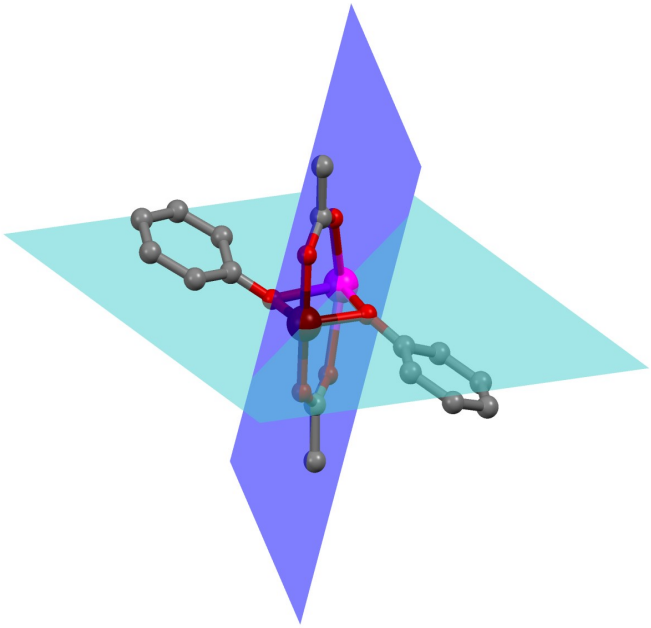

Fig. S1 Least square $CoDyO_2$ (phenoxido) and $CoDyC_2O_4$ (acetato) planes in **1** and **2**.

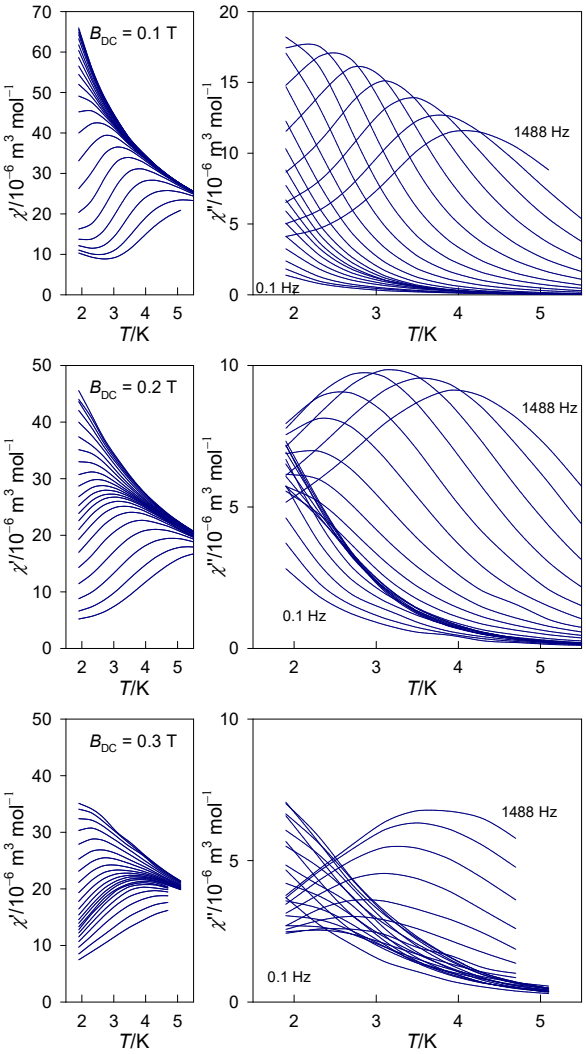

Fig. S2 Temperature dependence of the AC susceptibility components of **1** for various frequencies f = 0.1, 0.16, 0.25, 0.40, 0.63, 1.01, 1.58, 2.51, 3.98, 6.31, 10.01, 15.86, 25.11, 39.81, 63.09, 100.1, 158.4, 251.3, 398.9, 629.2, 997.3 and 1488 Hz.

Fitting of the AC susceptibility data is based upon 44 data points (22 in-phase and 22 out-of phase) using the explicit formulae for the two-component Debye model

a) in phase

$$\chi'(\omega) = \chi_S + (\chi_{T1} - \chi_S)\frac{1 + (\omega\tau_1)^{1-\alpha_1}\sin(\pi\alpha_1/2)}{1 + 2(\omega\tau_1)^{1-\alpha_1}\sin(\pi\alpha_1/2) + (\omega\tau_1)^{2-2\alpha_1}} + (\chi_{T2} - \chi_{T1})\frac{1 + (\omega\tau_2)^{1-\alpha_2}\sin(\pi\alpha_2/2)}{1 + 2(\omega\tau_2)^{1-\alpha_2}\sin(\pi\alpha_2/2) + (\omega\tau_2)^{2-2\alpha_2}}$$

b) out of phase

$$\chi''(\omega) = (\chi_{T1} - \chi_S)\frac{(\omega\tau_1)^{1-\alpha_1}\cos(\pi\alpha_1/2)}{1 + 2(\omega\tau_1)^{1-\alpha_1}\sin(\pi\alpha_1/2) + (\omega\tau_1)^{2-2\alpha_1}} + (\chi_{T2} - \chi_{T1})\frac{(\omega\tau_2)^{1-\alpha_2}\cos(\pi\alpha_2/2)}{1 + 2(\omega\tau_2)^{1-\alpha_2}\sin(\pi\alpha_2/2) + (\omega\tau_2)^{2-2\alpha_2}}$$

with the constraint for the isothermal susceptibilities $\chi_{T1} < \chi_{T2}$ in order to get positive contributions from each primitive component. Seven free parameters can be retrieved reliably by using 44 experimental data points.

The functional to be minimized accounts to the relative errors of both susceptibility components

- $F = w \cdot E(\chi') + (1 - w) \cdot E(\chi'')$ with the typical weight w = 0.07, or

- $F = E(\chi') \cdot E(\chi'')$ with

$$E(\chi) = (1/N)\left[\sum_i^N \left|(\chi_i^e - \chi_i^c)/\chi_i^e\right|\right]$$

The optimization routine refers to the genetic algorithm of D. L. Carroll, Univ. Illinois, Urbana, USA, 1998.

The quality of the fit is expressed by

a) discrepancy factors for the in-phase and out-of phase susceptibilities $R(\chi')$ and $R(\chi'')$ defined as

$$R(\chi) = \sqrt{\left[\sum_i (\chi_i^e - \chi_i^c)^2\right] / \left[\sum_i (\chi_i^e)^2\right]}$$

b) by the standard deviation for each optimized parameter; this is given in parentheses, e.g. 12.3(45) means 12.3 ± 4.5 (at 95% probability level).

The retrieved parameters should follow a systematic trend along a smooth dependence.

Table S2 Fitted parameters of the Debye model for **1** at B_{DC} = 0.1 T.

T/K	$R(\chi')$ /%	$R(\chi'')$ /%	χ_S	χ_{T1}	α_1	τ_1 /10^{-3} s	χ_{T2}	α_2	τ_2 /10^{-3} s
1.9	0.57	2.1	8.51(19)	20.5(12)	0.25(4)	85.0(100)	66.5(3)	0.18(1)	2.32(6)
2.3	0.48	1.9	7.39(15)	13.7(6)	0.22(5)	93.8(100)	56.5(2)	0.14(1)	1.45(2)
2.7	0.22	2.7	7.50(15)	11.4(4)	0.25(7)	100(14)	49.0(2)	0.09(1)	0.871(7)
3.1	0.33	4.1	7.50(23)	9.78(51)	0.24(13)	125(33)	43.5(2)	0.06(1)	0.520(6)
3.5	0.37	5.3	7.57(34)	8.85(55)	0.19(23)	165(74)	38.7(2)	0.04(1)	0.321(5)
3.9	0.53	1.4	6.25(27)	7.00(36)	0.18(20)	210(84)	35.3(1)	0.05(1)	0.194(3)
4.3	0.19	1.8	6.50(21)	6.91(25)	0.13(18)	263(89)	32.1(1)	0.06(1)	0.132(2)
4.7	0.11	2.9	7.11(36)	7.37(40)	0.13(32)	325(207)	29.6(1)	0.05(1)	0.0956(22)
5.1	0.31	0.59	7.42(38)	7.57(40)	0.06(38)	367(248)	27.4(1)	0.04(1)	0.0736(19)

Table S3 Fitted parameters of the Debye model for **1** at B_{DC} = 0.2 T.

T/K	$R(\chi')$ /%	$R(\chi'')$ /%	χ_S	χ_{T1}	α_1	τ_1 /10^{-3} s	χ_{T2}	α_2	τ_2 /10^{-6} s
1.9	0.85	1.5	1.09(37)	26.0(9)	0.34(1)	100(4)	48.1(3)	0.26(2)	477(16)
2.3	0.40	1.4	0.90(20)	17.2(5)	0.32(1)	93.8(26)	42.6(1)	0.25(1)	437(7)
2.7	0.28	0.86	1.40(12)	12.5(3)	0.34(1)	87.5(23)	38.1(1)	0.19(1)	354(3)
3.1	0.24	0.78	1.69(11)	8.72(20)	0.34(1)	110(3)	34.3(1)	0.17(1)	272(2)
3.5	0.22	0.92	1.50(13)	5.59(19)	0.27(2)	146(5)	30.9(1)	0.17(1)	200(2)
3.9	0.26	0.80	1.86(17)	4.70(23)	0.33(3)	162(10)	28.3(1)	0.14(1)	147(2)
4.3	0.20	0.93	1.93(19)	3.78(24)	0.34(3)	169(14)	25.9(1)	0.14(1)	107(1)
4.7	0.18	1.1	1.38(30)	2.77(36)	0.44(5)	177(27)	24.0(1)	0.14(1)	74.0(16)
5.1	0.26	1.5	1.66(59)	2.77(69)	0.50(8)	122(35)	22.3(1)	0.11(1)	54.8(25)
5.5	0.17	1.6	1.49(76)	2.52(90)	0.60(9)	56.3(227)	20.9(1)	0.10(1)	39.0(25)

Table S4 Fitted parameters of the Debye model for **1** at B_{DC} = 0.3 T.

T/K	$R(\chi')$ /%	$R(\chi'')$ /%	χ_S	χ_{T1}	α_1	τ_1 /10^{-3} s	χ_{T2}	α_2	τ_2 /10^{-6} s
1.9	0.61	2.6	0	25.4(3)	0.36(1)	169(3)	38.7(2)	0.37(1)	82.5(30)
2.3	0.52	2.4	0	20.4(3)	0.35(1)	143(3)	36.6(1)	0.35(1)	88.6(21)
2.7	0.40	2.0	0	15.5(2)	0.36(1)	125(3)	34.1(1)	0.31(1)	84.4(13)
3.1	0.41	2.3	0	10.9(2)	0.34(1)	141(4)	31.5(1)	0.29(1)	80.9(10)
3.5	0.41	2.6	0	7.35(16)	0.31(2)	160(6)	29.0(1)	0.27(1)	68.7(8)
3.9	0.39	2.0	0	5.10(14)	0.32(2)	189(9)	26.9(1)	0.25(1)	57.8(6)
4.3	0.38	2.1	0	3.54(16)	0.38(3)	202(17)	24.9(1)	0.22(1)	46.7(5)
4.7	0.27	2.6	0	2.94(17)	0.46(3)	247(33)	23.5(1)	0.19(1)	37.3(4)
5.1	0.10	2.6	0	1.53(9)	0.31(3)	281(16)	21.6(1)	0.30(5)	25.3(79)

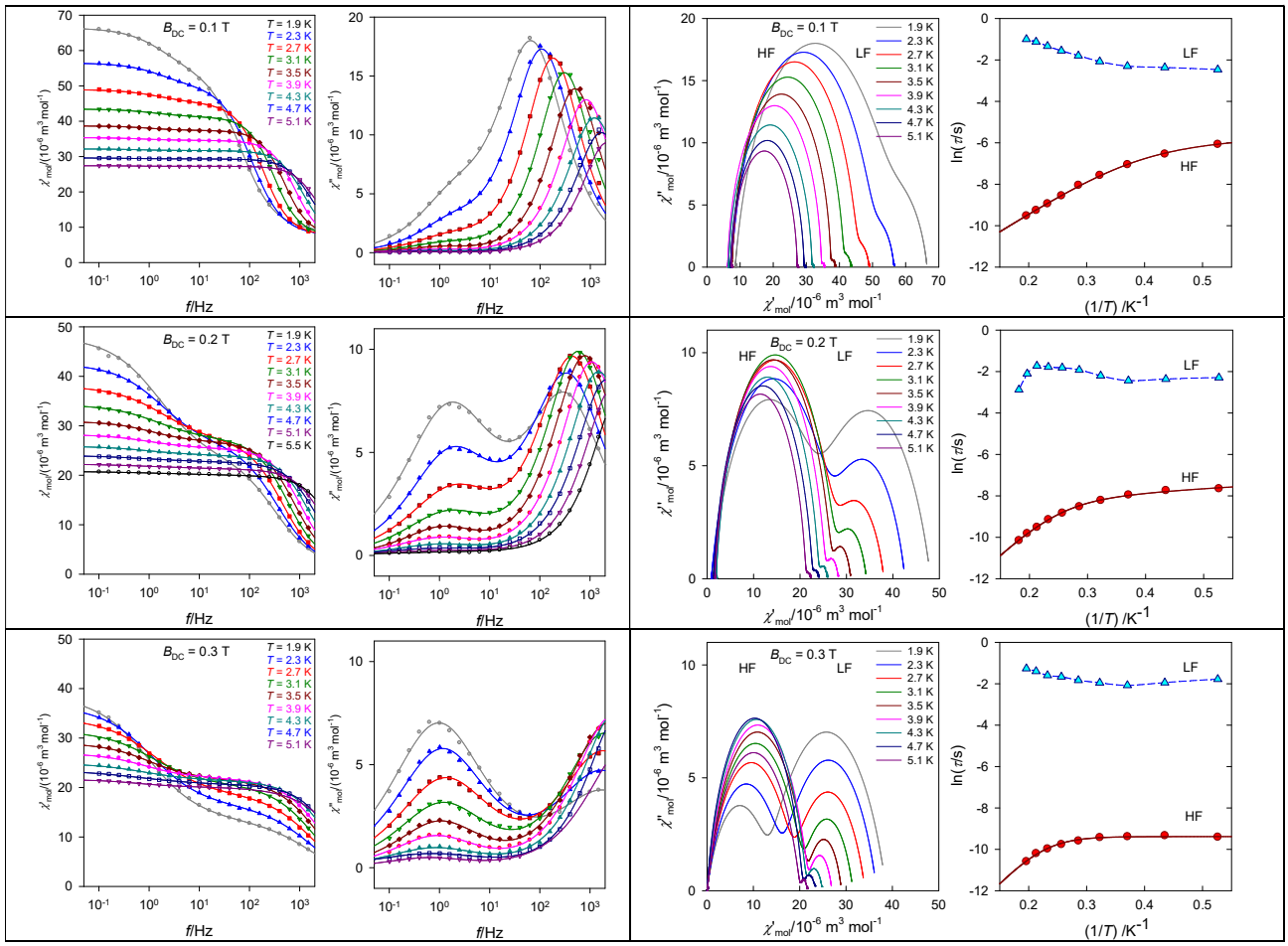

Fig. S3 Comparison of AC susceptibility data for **1** at different external magnetic field. Some trends:

- With increasing DC field the adiabatic susceptibility decreases (for $B_{DC} = 0.3$ it was fixed to $\chi_S = 0$).
- With increasing DC-field the height of the LF peak increases.
- With increasing DC-field the HF peak moves to higher frequencies (and outside the hardware limit) so that the corresponding relaxation times are shorter.
- With increasing DC-field the slope of the Arrhenius-like plot decreases and the $\ln \tau$ *vs* T^{-1} curve becomes more flat (temperature independent).
- With increasing temperature the maximum of the LF peak moves to lower frequencies that causes that the corresponding relaxation time increases (unusual behaviour).
- With increasing temperature the height of the LF peak disappears.

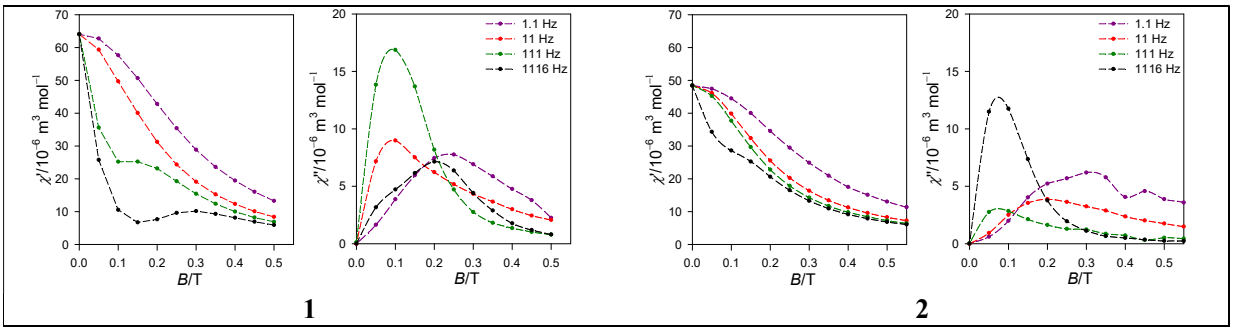

Fig. S4 Comparison of the field dependence of the AC susceptibility components for a set of frequencies at $T = 2.0$ K

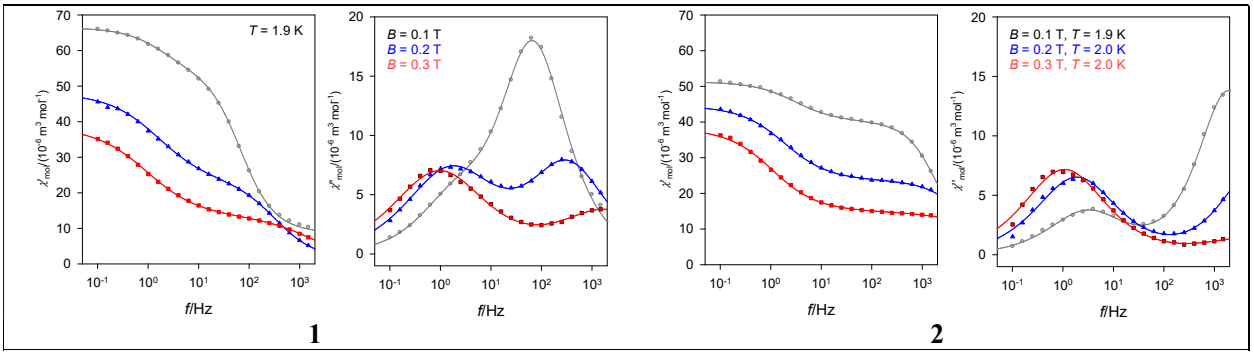

Fig. S5 Comparison of the frequency dependence of the AC susceptibility components for a set of external fields at $T = 1.9$ and/or 2.0 K.

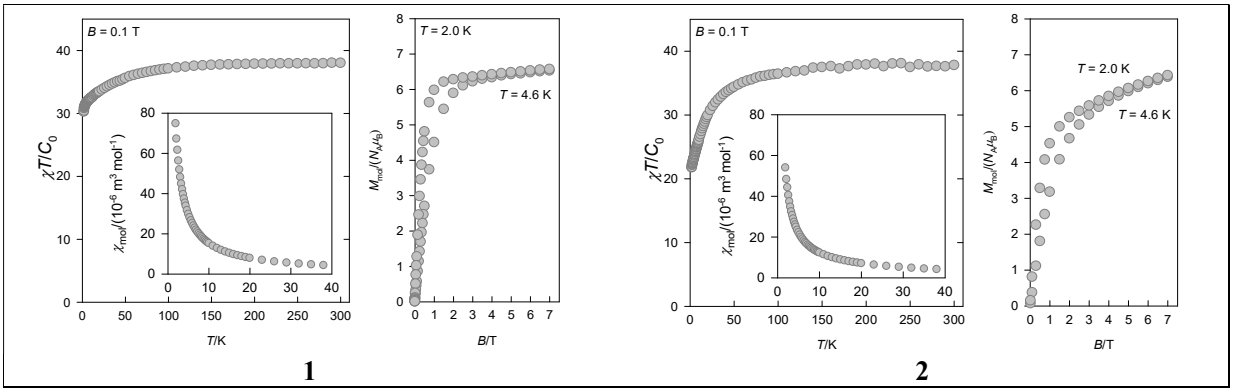

Fig. S6 Comparison of DC magnetic data for **1** and **2**.

Table S5 Crystallographic data of **1** and **2**.

	1	**2**
Formula	$C_{22}H_{24}N_2O_{14}CoDy$	$C_{24}H_{28}N_4O_{14}CoDy$
FW	789.88	817.93
Crystal system	Monoclinic	Monoclinic
Space group	*P*21/*n*	*P*21/*n*
a/Å	10.7189(9)	11.029(2)
b/Å	15.8478(14)	14.281(3)
c/Å	16.4828(15)	18.943(4)
β/°	98.315(3)	96.809(7)
V/Å^3	2770.5 (4)	2962.6(10)
Z	4	4
T/K	303(2)	303(2)
θ/°	2.437 – 30.607	2.344 – 25.773
μ (Mo Kα)/mm^{-1}	3.351	3.137
D_{calcd}/g cm^{-3}	1.894	1.834
F(000)	1556	1620
Index ranges	–15<*h*<15	–13<*h*<13
	–22<*k*<20	–16<*k*<17
	–23<*l*<23	–23<*l*<23
Rfs. collected	77261	65720
Rfs. unique/observed	7180 / 8505	4186 / 5656
R_{int}	0.0293	0.1148
R_1^a/ wR_2^b [I > 2ó(I)]	0.0235/0.0488	0.0317/0.0515
R_1^a/ wR_2^b [for all F_o^2]	0.0342/0.0529	0.0610/0.0582
GOF on F^2	1.077	1.034